THE JOURNAL OF PHYSICAL CHEMISTRY B

Article

pubs.acs.org/JPCB

Hydrogen-Atom Abstraction from a Model Amino Acid: Dependence on the Attacking Radical

Ruth I. J. Amos,*[,†,§] Bun Chan,*[,†,§] Christopher J. Easton,[‡,§] and Leo Radom*[,†,§]

[†]School of Chemistry, The University of Sydney, Sydney, NSW 2006, Australia

[‡]Research School of Chemistry, The Australian National University, Canberra, ACT 0200, Australia

[§]ARC Centre of Excellence for Free Radical Chemistry and Biotechnology

Supporting Information

ABSTRACT: We have used computational chemistry to examine the reactivity of a model amino acid toward hydrogen abstraction by HO•, HOO•, and Br•. The trends in the calculated condensed-phase (acetic acid) free energy barriers are in accord with experimental relative reactivities. Our calculations suggest that HO• is likely to be the abstracting species for reactions with hydrogen peroxide. For HO• abstractions, the barriers decrease as the site of reaction becomes more remote from the electron-withdrawing α-substituents, in accord with a diminishing polar deactivating effect. We find that the transition structures for α- and β-abstractions have additional hydrogen-bonding interactions, which lead to lower gas-phase vibrationless electronic barriers at these positions. Such favorable interactions become less important in a polar solvent such as acetic acid, and this leads to larger calculated barriers when the effect of solvation is taken into account. For Br• abstractions, the α-barrier is the smallest while the β-barrier is the largest, with the barrier gradually becoming smaller further along the side chain. We attribute the low barrier for the α-abstraction in this case to the partial reflection of the thermodynamic effect of the captodatively stabilized α-radical product in the more product-like transition structure, while the trend of decreasing barriers in the order $\beta > \gamma > \delta \sim \varepsilon$ is explained by the diminishing polar deactivating effect. More generally, the favorable influence of thermodynamic effects on the α-abstraction barrier is found to be smaller when the transition structure for hydrogen abstraction is earlier.

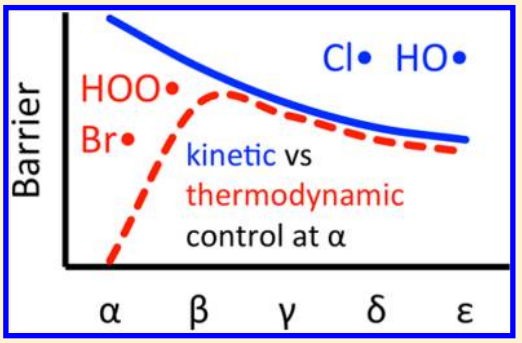

INTRODUCTION

Hydrogen-atom abstraction from amino acid derivatives, which represent structural motifs of the fundamental building blocks of peptides, is a critical event that may lead to damage to proteins.[1] In particular, abstraction from the α-position and the subsequent fragmentation have been identified as important steps in the development of a wide range of pathological conditions such as aging, cancer, and neurodegenerative disorders.[2]

Previous experimental and theoretical studies have found that abstraction of an α-hydrogen from an amino acid by Cl• is relatively unfavorable,[3−6] despite the fact that the carbon-centered radical product is thermodynamically stabilized by the captodative effect.[7−9] The associated larger reaction barrier has been attributed to a polar deactivating effect in the transition structure, which is found to be quite early,[5] resulting from the unfavorable interaction between the electrophilic Cl• and electron-withdrawing groups within the substrate.[3,5] The consequence is that hydrogen abstraction by Cl• generally occurs more readily from the side chain of an amino acid than from the thermodynamically preferred α-carbon.

What is the situation for radicals that are more directly relevant to biological systems? In this regard, the hydroxyl radical (HO•) is particularly pertinent. Under biological conditions, the α-hydrogens on peptide backbones are also found to be less reactive to HO• than those on the side chains, with the lower reactivity again attributed to polar deactivating effects.[3,6] However, the polar effects are slightly smaller for HO• than for Cl•. In contrast, the related *t*-BuO• radical has been found experimentally to abstract hydrogen preferentially from the α- and β-carbon positions of amino acids.[3]

Clearly, the nature of the abstracting radical alters the regioselectivity of hydrogen abstraction from amino acid species, which is in contrast to a recent proposal that the findings for HO• can be applied directly to other typical radical species.[10] Further evidence for the dependence on the radical can be seen from the preference for Br• to abstract from the α-carbon of amino acids.[3] It has been proposed that Br• abstraction is governed predominantly by the thermodynamic stability of the product radical, which would favor the formation of the α-radical due to captodative stabilization.[3]

In the present study, we use computational quantum chemistry to obtain further information concerning hydrogen abstraction from model amino acid derivatives (**1** and **2**, Figure

Special Issue: William L. Jorgensen Festschrift

Received: May 28, 2014
Revised: July 16, 2014

   dx.doi.org/10.1021/jp505217q | J. Phys. Chem. B XXXX, XXX, XXX−XXX

1). As with our previous study,[5] the use of **1** enables us to compare directly the reactivity of CH_2 moieties and focus on the influence of polar substituents in different positions. We have examined the reactivities of three different radicals, namely, HO•, HOO•, and Br•, that span a range of electrophilicities, in order to probe the dependence on the abstracting radical. The present study thus complements our previous results for Cl•,[5] and it extends our previous study of HO• abstraction[6] to the amino acid derivatives **1** and **2**.

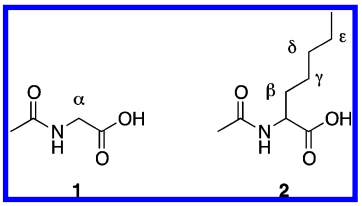

Figure 1. Model amino acid derivatives employed in the present study.

COMPUTATIONAL DETAILS

Standard ab initio molecular orbital theory and DFT calculations[11,12] were carried out with Gaussian 09.[13] We have used a theoretical approach that we have found previously to yield kinetics information with reasonable accuracy.[14,15] Gas-phase geometries of stationary points were obtained with the BHandH-LYP/6-31+G(d,p) procedure. Following each geometry optimization, harmonic frequency analysis was carried out to confirm the nature of each stationary point as an equilibrium structure or a transition structure. Improved single-point energies were evaluated using the B2K-PLYP procedure[16] in conjunction with the aug′-cc-pV(T+d)Z basis set, where aug′ denotes the use of diffuse functions only on non-hydrogen atoms. The frozen-core approximation was used in all B2K-PLYP calculations. Literature spin−orbit corrections of 0.83 and 14.70 kJ mol^{-1} were applied for HO• and Br•, respectively.[17] For comparison, the spin−orbit correction for Cl• is 3.52 kJ mol^{-1}.

To obtain the zero-point vibrational energies (ZPVEs) and thermal corrections for enthalpies (ΔH_{298}) and entropies (S_{298}) at 298 K, we used BHandH-LYP/6-31+G(d,p) harmonic vibrational frequencies and appropriate literature scale factors.[18] For nonstationary points on the reaction paths, the vibrations that correspond to the reaction coordinate are removed from the evaluation of ZPVEs, and ΔH_{298} and S_{298} values. For some nonstationary structures, harmonic vibrational analysis yields contentious low or imaginary frequencies. In those cases, the questionable frequencies are replaced by interpolated values obtained using formulas proposed by Truhlar and co-workers.[19]

The intrinsic reaction coordinate (IRC) procedure[20] was used to obtain reaction paths that connect transition structures with their adjacent minima. We employ the IRCmax method[21] to approximate a high-level reaction path, by carrying out high-level (B2K-PLYP) single-point energy calculations on a low-level (BHandH-LYP) IRC. Solvation corrections at each point on the reaction path were obtained at the M05-2*X*/6-31G(d) level using the SMD model.[22] In our previous study on Cl• abstractions,[5] the parameters for acetic acid were used in the SMD calculations to reflect the conditions of a closely related experimental study.[4] Such a choice is also adopted in the present investigation to enable a direct comparison with ref 5. The protocol of the SMD continuum model used in conjunction with the M05-2*X*/6-31G(d) procedure has been shown to provide a fairly accurate means for the calculation of solvation energies, with a mean absolute deviation from experiment of 2.7 kJ mol^{-1} for a large set of 2072 data points of neutral species in nonaqueous solvents.[22] For each type of the quantity examined, namely, the vibrationless energy (ΔE), 298 K enthalpy (ΔH), 298 K gas-phase free energy (ΔG_{gas}), and 298 K condensed-phase free energy (ΔG_{AcOH}), the transition structure is taken as the highest point on the respective IRCmax reaction path.

RESULTS AND DISCUSSION

Overall Trends. In our previous investigation of hydrogen abstraction by Cl•, we examined a series of amino-acid-related substrates. In particular, these included the N-acetyl amino acid derivatives (**1** and **2**) as models for a residue in a peptide, and these will be the focus of the present study. The relatively long side chain in **2** (four CH_2 units) enables us to examine the effect of distal substituents on the thermodynamics and kinetics of the hydrogen-abstraction reactions. As in previous work, in order to allow a direct comparison between the reactivity at the α-carbon and those for side-chain CH_2 units, we use the glycine analogue **1** as our model for an α-CH_2. We expect the N-acetyl group to be mildly electron-withdrawing due to the acetyl moiety being σ-electron-withdrawing, with the electron-donating lone-pair of the amino group tied up through the π system.

The condensed-phase (acetic acid) free energy barriers and the corresponding reaction free energies for the abstraction by Cl•, HO•, HOO•, and Br• are shown in Table 1. The trends

Table 1. Condensed-Phase (Acetic Acid) Free Energy Barriers and Reaction Free Energies (kJ mol^{-1}) for Hydrogen Abstraction by the Various Radicals

	Cl•[a]	HO•	HOO•	Br•
		Free Energy Barrier		
α	31.3	51.5	108.8	37.0
β	26.2	48.7	119.8	60.0
γ	25.3	46.4	116.3	56.2
δ	23.0	38.9	106.8	50.9
ε	23.0	39.0	109.8	42.3
		Reaction Free Energy		
α	−82.0	−154.0	−15.5	−28.9
β	−32.2	−104.2	+34.3	+20.9
γ	−32.1	−104.1	+34.4	+21.0
δ	−33.2	−105.2	+33.3	+19.9
ε	−34.6	−106.6	+31.9	+18.5

[a]Reference 5.

in the reaction free energies are the same for the four types of abstraction reactions, and are related to one another by the bond energies for H−Cl, H−OH, H−OOH, and H−Br. The α-abstractions have a considerably more negative reaction free energy, associated with the formation of the captodatively stabilized α-radical, than the abstractions from all the other positions, the latter leading to very similar reaction free energies. For the free energy barriers, for Cl• and HO•, the general trend with respect to the site of reaction is a decrease in the barrier in the order $\alpha > \beta > \gamma > \delta \sim \varepsilon$. On the other hand, for HOO• and Br•, the barrier associated with β-abstraction is the largest, with a generally gradual decrease observed as the

dx.doi.org/10.1021/jp505217q | J. Phys. Chem. B XXXX, XXX, XXX−XXX

reaction moves further away from the β-position, i.e., $\alpha < \beta > \gamma > \delta \sim \varepsilon$.

Thus, it appears that abstractions by Cl• and HO• show a contrathermodynamic behavior such that α-abstraction, which is thermodynamically most favorable, is associated with the largest free energy barrier. On the other hand, the smaller α-barriers for HOO• and Br• abstractions are more in line with thermodynamics. As discussed earlier, the observation of contrathermodynamic behavior has been rationalized by unfavorable polar effects developed in the transition structures.[3,5] Therefore, on the basis of the free energy barriers and reaction free energies presented in Table 1, one may argue that such a polar effect is prominent for abstractions by Cl• and HO•, but it is relatively less important for HOO• and Br• abstractions. However, as we shall see, while calculated relative free energies in acetic acid arguably represent the quantity that is most relevant to the experimental abstraction process, there are subtle considerations that are required to obtain a more complete understanding.

We will proceed to examine in more detail the variations in the components that contribute to the free energy barrier in acetic acid. Thus, we have investigated the barriers on the vibrationless reaction path ($\Delta E^{\ddagger}$), as well as the 298 K gas-phase enthalpy barriers ($\Delta H^{\ddagger}$), the 298 K gas-phase free energy barriers ($\Delta G^{\ddagger}_{gas}$), and the 298 K condensed-phase free energy barriers ($\Delta G^{\ddagger}_{AcOH}$). The various types of calculated barriers for the reactions of HO•, HOO•, and Br• are summarized in Table 2.

Table 2. Vibrationless Barriers, 298 K Gas-Phase Enthalpy Barriers, and 298 K Free Energy Barriers (Gas and Condensed Phase) (kJ mol^{-1})

	$\Delta E^{\ddagger}$	$\Delta H^{\ddagger}$	$\Delta G^{\ddagger}_{gas}$	$\Delta G^{\ddagger}_{AcOH}$
		HO•		
α	−1.0	−2.9	40.1	51.5
β	7.0	4.6	42.5	48.7
γ	14.9	10.2	47.7	46.4
δ	11.8	8.3	43.9	38.9
ε	11.3	7.4	42.4	39.0
		HOO•		
α	70.0	59.9	104.3	108.8
β	76.7	66.0	112.7	119.8
γ	84.9	73.1	118.5	116.3
δ	83.5	71.8	110.6	106.8
ε	83.3	71.6	113.7	109.8
		Br•		
α	4.7	1.8	34.3	37.0
β	53.7	34.3	67.6	60.0
γ	43.8	25.5	58.0	56.2
δ	37.4	19.2	50.4	50.9
ε	39.9	22.0	48.7	42.3

Before we begin our discussion of $\Delta E^{\ddagger}$ through $\Delta G^{\ddagger}_{AcOH}$, it is noteworthy that, while the exact transition structure for each reaction depends on the type of reaction path used to characterize it, the differences in the structures and the associated energies are small and they do not affect the qualitative trends. Moreover, the transition structures that correspond to $\Delta E^{\ddagger}$ have similar geometries compared with the BHandH-LYP-optimized ones, which is in contrast to some Cl• abstractions for which the application of IRCmax leads to significantly earlier transition structures.[5,15] In a previous study,[15] we found that the transition structure for a Cl• abstraction reaction that has a larger barrier is usually less affected by IRCmax than one that has a smaller barrier. To this end, we note that abstractions by HO•, HOO•, and Br• generally have larger barriers than Cl• abstractions (Table 1), and this may explain the relative insensitivity of their transition structures to IRCmax. The larger barriers for HO• abstractions than those for Cl• abstractions, despite the former being more exergonic, are intriguing. However, it is consistent with the reactivity of CH_4 toward abstractions by Cl• and HO•, for which the former has a rate of 1.0×10^{-13} cm^3 molecule^{-1} s^{-1} while the latter has a slower rate of 6.3×10^{-15} cm^3 molecule^{-1} s^{-1}.[23]

HO• Abstractions. We can see that, while the free energy barriers in acetic acid ($\Delta G^{\ddagger}_{AcOH}$) for HO• abstraction gradually become smaller as one moves away from the α-carbon, this is not the case for $\Delta E^{\ddagger}$, $\Delta H^{\ddagger}$, and $\Delta G^{\ddagger}_{gas}$. In fact, abstraction from the α-position has the smallest barrier for all of these three quantities. The barriers initially become larger as the site of abstraction becomes more remote from α, reaching the largest values at γ, and then gradually decreasing.

To rationalize such a trend, which differs from the trend in $\Delta G^{\ddagger}_{AcOH}$, we have inspected the transition structures for the HO• abstraction (Figure 2). We note that, for the abstraction from the α- and the β-positions, the abstracting HO• appears to interact with one or both of the N-acetylamino and carboxylic acid substituents. However, we do not observe similar types of interactions for the transition structures at the γ-, δ-, and ε-positions. The additional attractive interactions in the transition structures for the α- and β-abstractions act in the opposite direction to the unfavorable polar effects, and this is consistent with their lower barriers. The hydrogen-bonding interactions are partly washed out in the condensed phase with a polar solvent such as acetic acid, and this leads to higher calculated barriers at the α- and β-positions. We note that, in a less polar solvent, namely, carbon tetrachloride, the effect of solvation is smaller such that α-abstraction no longer has the largest barrier, with the values of $\Delta G^{\ddagger}_{CCl_4}$ being 47.7 (α), 48.6 (β), 53.4 (γ), 45.8 (δ), and 45.4 (ε) kJ mol^{-1}. At the other end of the spectrum, we have obtained $\Delta G^{\ddagger}_{H_2O}$ values of 58.5 (α), 54.5 (β), 50.8 (γ), 40.4 (δ), and 41.2 (ε) kJ mol^{-1}. The involvement of hydrogen bonding in the abstractions at the α- and β-positions may require the use of explicit solvent molecules in the calculations for a more quantitative description. However, this is beyond the scope of the present study. As we shall put forward shortly, our rationalization for polar effects is based mostly on abstractions that are not complicated by additional hydrogen bonding, and we deem the use of the generally accurate SMD continuum model adequate under such circumstances.

The transition structures for γ- through ε-abstractions do not show hydrogen-bonding interactions, so the trends for these three barriers provide a useful indicator for polar effects. The mild decrease in barriers as the abstractions move further away from the α-substituents is consistent with the electrophilic nature of HO• and an unfavorable polar effect in the transition structure associated with the electron-withdrawing nature of the N-acetylamino and carboxylic acid substituents. In particular, this is observed for the simplest of our calculated barriers, $\Delta E^{\ddagger}$, as might have been expected for the electronic polar effect. As an aside, we note that both HO• and Cl• abstractions are quite reactant-like (e.g., C···H in the transition structures for α-

dx.doi.org/10.1021/jp505217q | J. Phys. Chem. B XXXX, XXX, XXX−XXX

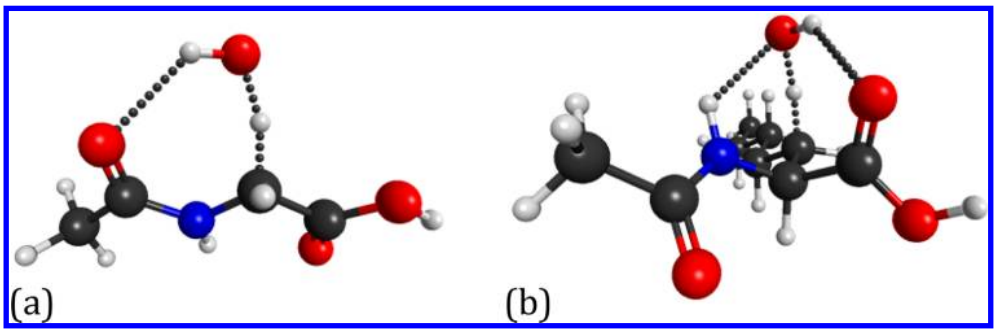

Figure 2. Transition structures for hydrogen abstraction by HO• from the (a) α-position showing an OH···O═CCH_3 hydrogen bond and (b) β-position showing OH···O═COH and HO···HN hydrogen bonds.

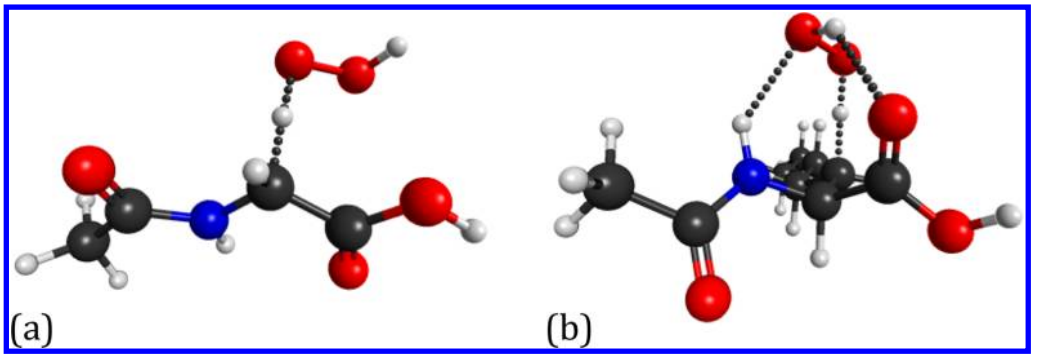

Figure 3. Transition structures for hydrogen abstraction by HOO• from the (a) α-position and (b) β-position showing in the latter case OOH···O═COH and O—(H)O···HN hydrogen bonds.

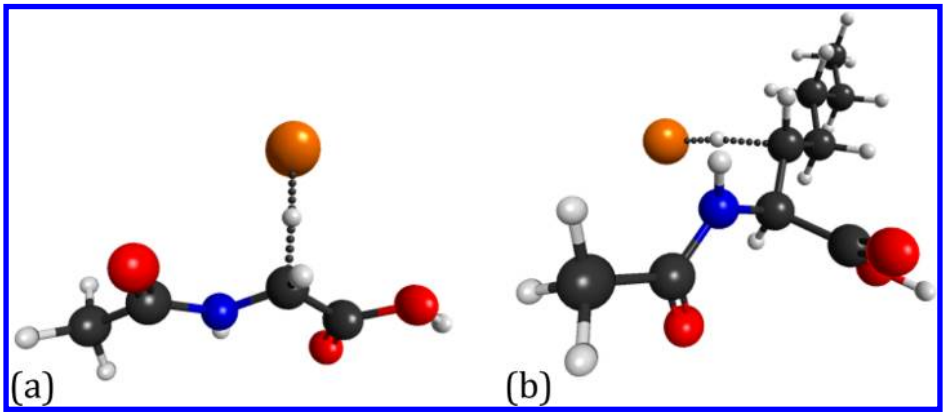

Figure 4. Transition structures for hydrogen abstraction by Br• from the (a) α- and (b) β-positions.

abstractions by HO• and Cl• are 1.227 and 1.202 Å, respectively), and this is compatible with their barriers being relatively insensitive to thermodynamic effects when compared with HOO• and (especially) Br• abstractions, as we shall see.

HOO• Abstractions. For the reactions with HOO•, we also find that the transition structures for the β-abstraction are associated with hydrogen-bonding interactions between HOO• and the α-substituents (Figure 3b). These interactions contribute to the generally lower $\Delta E^{\ddagger}$, $\Delta H^{\ddagger}$, and $\Delta G^{\ddagger}_{gas}$ values at the β-position than those for γ-, δ-, and ε-abstractions. However, the effect of solvation leads to a larger $\Delta G^{\ddagger}_{AcOH}$ for β-abstraction than those for reactions further down the side chain because the stabilizing effect of hydrogen-bonding interactions is reduced in acetic acid.

For the α-abstraction by HOO• (Figure 3a), in contrast to the analogous HO• abstraction (Figure 2a), we do not find a hydrogen-bonded transition structure despite numerous attempts to locate one. Nevertheless, the α-abstraction has the lowest $\Delta E^{\ddagger}$, perhaps associated with partial captodative stabilization in the transition structure, which is found to be quite late (see below). The absence of hydrogen bonding in the α-abstraction transition structure means that this observation is not strongly affected by solvation.

We now examine in more detail the $\Delta E^{\ddagger}$ values for the HOO• abstractions. It can be seen that, for the reactions at the γ-, δ-, and ε-positions, the vibrationless barriers are comparable to one another. Thus, it appears that for abstraction by HOO• any unfavorable polar effect is relatively small, such that it has diminished significantly upon reaching the γ-position. Furthermore, the observation that the α-$\Delta E^{\ddagger}$ is the lowest, despite the absence of additional attractive hydrogen-bonding interactions, shows that any polar effect, if present, is overshadowed by the thermodynamics associated with the product radical. To this end, we note that HOO• abstraction at the α-position has

dx.doi.org/10.1021/jp505217q | J. Phys. Chem. B XXXX, XXX, XXX–XXX

a transition structure that is somewhat more product-like (C···H = 1.301 Å) than that for the corresponding HO• abstraction (C···H = 1.227 Å), which is consistent with the HOO• α-abstraction being more affected by product thermodynamics than the abstraction by HO•.

Br• Abstractions. For Br• abstractions, the α-barriers are the smallest regardless of the type of barrier considered, i.e., $\Delta E^{\ddagger}$, $\Delta H^{\ddagger}$, $\Delta G^{\ddagger}_{gas}$, or $\Delta G^{\ddagger}_{AcOH}$. The general trend for β-, γ-, δ-, and ε-abstraction barriers for the four quantities is $\beta > \gamma > \delta \sim \varepsilon$. We do not see the existence of hydrogen-bonding interactions for abstractions from any of the positions (e.g., see the α- and β-abstraction transition structures, Figure 4), as we also found to be the case for Cl• abstractions.[5] As a result, we can presume in this case that $\Delta E^{\ddagger}$ would be a reasonable and unbiased indicator for thermodynamic as well as polar effects experienced in the transition structures for the abstractions at all positions.

Thus, the gradual decrease in the barrier $\beta > \gamma > \delta \sim \varepsilon$ reflects the unfavorable polar effect experienced in the transition structures, which becomes smaller as the reaction center moves away from the electron-withdrawing α-substituents. The lower α-$\Delta E^{\ddagger}$ suggests that the favorable thermodynamic effect of a captodatively stabilized α-radical product overshadows the unfavorable polar effect in the transition structure. The considerable influence of the thermodynamics of the product radical on α-$\Delta E^{\ddagger}$ is consistent with the transition structure being significantly more product-like, with a C···H distance of 1.388 Å. We reiterate that the trend of $\alpha \ll \beta > \gamma > \delta \sim \varepsilon$ is observed for all of the different types of barriers $\Delta E^{\ddagger}$, $\Delta H^{\ddagger}$, $\Delta G^{\ddagger}_{gas}$, and $\Delta G^{\ddagger}_{AcOH}$. In particular, the trends for $\Delta G^{\ddagger}_{gas}$ and $\Delta G^{\ddagger}_{AcOH}$ are the same. Thus, we can see that, in the absence of additional hydrogen-bonding interactions in the transition structure, the effect of solvation does not appear to modify the regioselectivity of the abstraction reactions.

Comparison with Experiment. Our calculated condensed-phase (acetic acid) free energy barriers, including those of a previous study,[5] are compared with observed relative reactivities for experiments with chlorine and hydrogen peroxide reported by Watts and Easton[4] in Table 3. In our previous study,[5] we had already noted that the gradual decrease in condensed-phase barriers along the side chain for Cl• abstraction is consistent with the experimental observation of increasing reactivity in the same order, and such an agreement is reinforced here.

For experiments with hydrogen peroxide (H_2O_2), we note that both HO• and HOO• are potential reactive radicals. In the present study, our calculations indicate that the barriers for HOO• abstractions are substantially greater than those for the abstractions by HO• (Table 1). This is consistent with the greatly reduced exothermicity (or even endothermicity) of the HOO• abstractions. Thus, it is likely that HO• is the abstracting radical in the reaction with H_2O_2. Under physiological conditions, deprotonation of HOO• gives the superoxide radical anion $•O_2^-$. However, it is generally even less reactive than HOO•,[2] and is therefore less relevant in terms of hydrogen-atom abstraction. In a similar manner to Cl• abstractions, the reactivity with hydrogen peroxide is notably smaller at the β-position than further down the side chain. The calculated $\Delta G^{\ddagger}_{AcOH}$ (HO•) values obtained in the present study, which decrease in the order $\alpha > \beta > \gamma > \delta \sim \varepsilon$ (Table 3), are consistent with the experimental observations.

For Br• abstractions, there have been numerous studies showing that reactions with amino acid derivatives generally occur exclusively at the α-position.[3] This is consistent with our computational result that α-abstraction is highly favored for the reaction with Br• (Table 1). Ultimately, the partial captodative stabilization of an α-transition structure provides a strong driving force for reactions with Br• because of the late transition structure. As an example, bromination of PhC(O)-NH−CH_2−CO_2Me occurs at the CH_2 moiety and is found to be at least 2 orders of magnitude faster than the analogous reactions for PhC(O)NH−CH_2−CH_3 and CH_3−CH_2−CO_2Me,[3] i.e., substrates that contain only one of the capto or dative groups.

Table 3. Experimental Relative Reactivities[a] and Calculated Condensed-Phase (Acetic Acid) Free Energy Barriers (kJ mol^{-1})[b,c] for Hydrogen Abstractions from CH_2 and CH_3 Groups

	CH_2	CH_3	CH_2	CH_3
	Reactivity (Chlorine)		Reactivity (Hydrogen Peroxide)	
α	0.20			
β	0.35	0.03		0.02
γ	2.70	0.45		0.12
δ	5.00	1.30		0.17
ε		2.00		0.12
	$\Delta G^{\ddagger}_{AcOH}$ (Cl•)[b]		$\Delta G^{\ddagger}_{AcOH}$ (HO•)[c]	
α	31.3		51.5	
β	26.2		48.7	
γ	25.3		46.4	
δ	23.0		38.9	
ε	23.0		39.0	

[a]Reference 4. [b]Reference 5. [c]Present work.

CONCLUDING REMARKS

In the present study, we have used computational chemistry to examine the reactivity of a model amino acid residue toward hydrogen abstraction by HO•, HOO•, and Br•, to complement our previous investigation of Cl• abstraction for the same system. The trends in the calculated free energy barriers in acetic acid are in accord with experimental relative reactivities for reactions with chlorine, hydrogen peroxide, and bromine, with our calculations suggesting that HO• rather than HOO• is likely to be the abstracting species for the hydrogen peroxide reactions. Thus, for Cl• and HO• abstractions, the barriers decrease as the site of reaction becomes more remote from the electron-withdrawing α-substituents. On the other hand, for Br• abstractions, the α-barrier is the smallest while the β-barrier is the largest, with the barrier becoming smaller further down the side chain.

The trend in the Cl• reaction was attributed in our previous study to a polar deactivating effect in the transition structure, which was found to be early. While the trend in the condensed-phase free energy barrier for HO• abstractions is similar to that for Cl• and therefore appears to be entirely attributable to a polar effect, an examination of the underlying vibrationless electronic barriers reveals a more complex situation. A comparison of the barriers for side-chain abstractions at the γ-, δ-, and ε-positions indeed shows that HO• abstractions are sensitive to polar effects. However, in the gas phase, abstractions from the α- and β-positions, which can be expected to be influenced the most by polar deactivation,

dx.doi.org/10.1021/jp505217q | J. Phys. Chem. B XXXX, XXX, XXX−XXX

actually have lower electronic barriers. This contrasting observation results from the presence of additional hydrogen-bonding interactions in the α- and β-transition structures. Such interactions become partly washed out and are therefore less important in a polar solvent such as acetic acid, and this leads to larger α- and β-barriers as a result of the now dominant polar deactivating effects.

For the abstraction reactions by Br•, the nonmonotonic trend in the barriers can be attributed to two effects. The low barrier for the α-abstraction is in line with the thermodynamics for the generation of the captodatively stabilized α-radical, and suggests that such an effect is already partially reflected in the transition structure, which is found to be more product-like than the transition structures for the α-abstractions by Cl• and HO•. The trend of decreasing barriers in the order $\beta > \gamma > \delta \sim \epsilon$ can be attributed to a diminishing polar deactivation along the side chain. More generally, the influence of favorable thermodynamic effects on the α-abstraction barrier is greatest for Br• with its later transition structure and smallest for Cl• with its earlier transition structure.

■ ASSOCIATED CONTENT

Supporting Information

Optimized geometries of relevant species (Table S1); ZPVEs, thermal corrections to enthalpies, entropies, solvation energies, and high-level single-point energies (Table S2); and full citation for ref 13. This material is available free of charge via the Internet at http://pubs.acs.org.

■ AUTHOR INFORMATION

Corresponding Authors

*E-mail: ruth.amos@sydney.edu.au.
*E-mail: bun.chan@sydney.edu.au.
*E-mail: radom@chem.usyd.edu.au.

Notes

The authors declare no competing financial interest.

■ ACKNOWLEDGMENTS

We gratefully acknowledge funding (to L.R. and C.J.E.) from the Australian Research Council (ARC) and generous grants of computer time from the National Computational Infrastructure (NCI) National Facility and Intersect Australia Ltd.

■ REFERENCES

(1) Garrison, W. M. Reaction Mechanisms in the Radiolysis of Peptides, Polypeptides, and Proteins. *Chem. Rev.* **1987**, *87*, 381−398.
(2) Davies, M. J.; Dean, R. T. *Radical-Mediated Protein Oxidation: From Chemistry to Medicine*; Oxford University Press: New York, 1997.
(3) Easton, C. J. Free-Radical Reactions in the Synthesis of α-Amino Acids and Derivatives. *Chem. Rev.* **1997**, *97*, 53−82.
(4) Watts, Z. I.; Easton, C. J. Peculiar Stability of Amino Acids and Peptides from a Radical Perspective. *J. Am. Chem. Soc.* **2009**, *131*, 11323−11325.
(5) O'Reilly, R. J.; Chan, B.; Taylor, M. S.; Ivanic, S.; Bacskay, G. B.; Easton, C. J.; Radom, L. Hydrogen Abstraction by Chlorine Atom from Amino Acids: Remarkable Influence of Polar Effects on Regioselectivity. *J. Am. Chem. Soc.* **2011**, *133*, 16553−16559.
(6) Chan, B.; O'Reilly, R. J.; Easton, C. J.; Radom, L. Reactivities of Amino Acid Derivatives Toward Hydrogen Abstraction by •Cl and HO•. *J. Org. Chem.* **2012**, *77*, 9807−9812.
(7) Viehe, H. G.; Janousek, Z.; Merenyi, R.; Stella, L. The Captodative Effect. *Acc. Chem. Res.* **1985**, *18*, 148−154.
(8) Yu, D.; Rauk, A.; Armstrong, D. A. Radicals and Ions of Glycine: An Ab Initio Study of the Structures and Gas-Phase Thermochemistry. *J. Am. Chem. Soc.* **1995**, *117*, 1789−1796.
(9) Croft, A. K.; Easton, C. J.; Radom, L. Design of Radical-Resistant Amino Acid Residues: A Combined Theoretical and Experimental Investigation. *J. Am. Chem. Soc.* **2003**, *125*, 4119−4124.
(10) Scheiner, S.; Kar, T. Analysis of the Reactivities of Protein C−H Bonds to H Atom Abstraction by OH Radical. *J. Am. Chem. Soc.* **2010**, *132*, 16450−16459.
(11) Koch, W.; Holthausen, M. C. *A Chemist's Guide to Density Functional Theory*, 2nd ed.; Wiley: New York, 2001.
(12) Jensen, F. *Introduction to Computational Chemistry*, 2nd ed.; Wiley: Chichester, U.K., 2007.
(13) Frisch, M. J.; Trucks, G. W.; Schlegel, H. B.; Scuseria, G. E.; Robb, M. A.; Cheeseman, J. R.; Scalmani, G.; Barone, V.; Mennucci, B.; Petersson, G. A.; et al. *Gaussian 09*, revision C.03; Gaussian, Inc.: Wallingford, CT, 2009.
(14) Chan, B.; Radom, L. Assessment of Theoretical Procedures for Hydrogen-Atom Abstraction by Chlorine, and Related Reactions. *Theor. Chem. Acc.* **2011**, *130*, 251−260.
(15) Chan, B.; Radom, L. Approaches for Obtaining Accurate Rate Constants for Hydrogen Abstraction by a Chlorine Atom. *J. Phys. Chem. A* **2012**, *116*, 3745−3752.
(16) Tarnopolsky, A.; Karton, A.; Sertchook, R.; Vuzman, D.; Martin, J. M. L. Double-Hybrid Functionals for Thermochemical Kinetics. *J. Phys. Chem. A* **2008**, *112*, 3−8.
(17) Curtiss, L. A.; Raghavachari, K.; Redfern, P. C.; Rassolov, V.; Pople, J. A. Gaussian-3 (G3) Theory for Molecules Containing First and Second-Row Atoms. *J. Chem. Phys.* **1998**, *109*, 7764−7776.
(18) Merrick, J. P.; Moran, D.; Radom, L. An Evaluation of Harmonic Vibrational Frequency Scale Factors. *J. Phys. Chem. A* **2007**, *111*, 11683−11700.
(19) Hu, W.-P.; Liu, Y.-P.; Truhlar, D. G. Variational Transition-State Theory and Semiclassical Tunnelling Calculations with Interpolated Corrections: A New Approach to Interfacing Electronic Structure Theory and Dynamics for Organic Reactions. *J. Chem. Soc., Faraday Trans.* **1994**, *90*, 1715−1725.
(20) Hratchian, H. P.; Schlegel, H. B. In *Theory and Applications of Computational Chemistry: The First 40 Years*; Dykstra, C. E., Frenking, G., Kim, K. S., Scuseria, G., Eds.; Elsevier: Amsterdam, The Netherlands, 2005; pp 195−249.
(21) Petersson, G. A. In *Computational Thermochemistry: Prediction and Estimation of Molecular Thermodynamics*; Irikura, K. K., Frurip, D. J., Eds.; ACS Symposium Series 677; American Chemical Society: Washington, DC, 1998; pp 237−266.
(22) Marenich, A. V.; Cramer, C. J.; Truhlar, D. G. Universal Solvation Model Based on Solute Electron Density and a Continuum Model of the Solvent Defined by the Bulk Dielectric Constant and Atomic Surface Tensions. *J. Phys. Chem. B* **2009**, *113*, 6378−6396.
(23) IUPAC Evaluated Kinetic Data. http://iupac.pole-ether.fr (accessed May 2014).